Molecular and Electronic Structure of C 5 H 5 N −SO 3 : Correlation of Ground State Physical Properties with Orbital Energy Gaps in Partially Bound Lewis Acid−Base Complexes

ARTICLE *in* THE JOURNAL OF PHYSICAL CHEMISTRY A · JUNE 2001

Impact Factor: 2.69 · DOI: 10.1021/jp010460u

2 AUTHORS, INCLUDING:

Sherri W. Hunt
United States Environmental Protection Age…

24 PUBLICATIONS **629** CITATIONS

SEE PROFILE

Molecular and Electronic Structure of $C_5H_5N-SO_3$: Correlation of Ground State Physical Properties with Orbital Energy Gaps in Partially Bound Lewis Acid−Base Complexes

S. W. Hunt and K. R. Leopold*

Department of Chemistry, University of Minnesota, 207 Pleasant Street, SE, Minneapolis, Minnesota 55455

Received: February 7, 2001; In Final Form: March 28, 2001

The donor−acceptor complex $C_5H_5N-SO_3$ has been studied in the gas phase using rotational spectroscopy. The adduct has the expected geometry in which the nitrogen lone pair is directed along the C_3 axis of the SO_3 and the SO_3 undergoes free or nearly free internal rotation within the complex. The N−S bond length is 1.915(1) Å, and the NSO angle is 98.91(2)°, indicating that the formation of the dative bond is nearly, but not entirely, complete. Small but significant changes in the heavy-atom ring structure of the pyridine upon complexation are also measured by a series of ^{13}C substitution experiments. Analysis of the ^{14}N quadrupole coupling constants indicates a transfer of approximately 0.54 electrons away from the pyridine upon formation of the dative bond. In the series of complexes of SO_3 with HCN, CH_3CN, H_3N, C_5H_5N, and $(CH_3)_3N$, electron-transfer values increase as the bond length decreases, and these changes are shown to accompany a gradual decrease in the energy gap between the lone pair orbital of the base and the LUMO of SO_3. Tabulated values of hardness (η) and electronegativity (χ) give rough but irregular estimates of these energy gaps, and the best correlations are obtained with energies derived directly from ionization potentials for the pertinent orbitals. Binding energies (D_e) have also been determined for the following complexes at the MP2/aug-cc-pVTZ level of theory/basis set: $(CH_3)_3N-SO_3$ (36.3 kcal/mol), $C_5H_5N-SO_3$ (25.5 kcal/mol), H_3N-SO_3 (19.6 kcal/mol), CH_3CN-SO_3 (9.0 kcal/mol), $HCCCN-SO_3$ (7.4 kcal/mol), and $HCN-SO_3$ (7.3 kcal/mol). These values also correlate with the energy gap between the donor orbital of the base and the acceptor orbital of the SO_3.

Introduction

Structure and bonding in Lewis acid−base complexes has long been a subject of much chemical interest.[1] In our laboratory, recent work has focused on the investigation of such systems in which the dative linkages appear to be intermediate between van der Waals interactions and fully formed chemical bonds.[2] Although molecular structure has been the primary focus in these studies, supplementary data from nuclear hyperfine constants and Stark effect measurements has, in some cases, yielded additional information about electron distributions.[3−5] Thus, as a class, these complexes have both revealed an interesting structural chemistry and provided an unusual perspective on the evolution of molecular physical properties between the limits of van der Waals and chemical interactions.

The question of what dictates the extent of dative bond formation in partially bound adducts follows naturally from these studies. Clearly, notions of intrinsic strength and compatibility of the acid and base should be important, and basic chemical ideas relating to acidity and basicity are expected to apply. Perhaps the best known treatments of acid−base interactions involve the "E and C" parameters of Drago[6] and the principle of Hard and Soft Acids and Bases (HSAB),[7] though an interesting account,[7a] starting with early work by Schwarzenbach,[8] Ahrland et al.,[9] and Edwards[10] underscores a long history of work on the subject. Numerous computational studies have also been presented.[11]

Central to most simple theories of Lewis acidity is the idea that both ionic and covalent interactions play important roles in stabilizing the donor−acceptor bond. In the language of the HSAB principle, for example, ionic contributions dominate in so-called "hard−hard" complexes, while covalency underlies the binding in "soft−soft" interactions.[7,12] Molecular orbital pictures have also proven useful as, for example, in the quantification of chemical hardness given by Parr and Pearson in 1983,[13] and in Mulliken's treatment of weak charge-transfer complexes.[1c,14] In contrast with most theories of acids and bases, whose primary focus is energetics, our own work has been concerned with ground-state properties such as molecular and electronic structure. Nevertheless, in light of the appealing simplicity and broad success of acid−base theories in general, it seems reasonable to attempt to discuss these physical properties of partially bound systems in some similar context as well.

In this paper, we present a microwave spectroscopic investigation of the gas phase donor−acceptor complex formed from pyridine (py) and SO_3. The immediate motivation for this work stems from a recent study of the closely related system $(CH_3)_3N-SO_3$, in which aspects of the molecular and electronic structure were elucidated.[4] Although pyridine and $(CH_3)_3N$ are of similar basicity, as judged by proton affinities,[15] pyridine is significantly softer.[7d] Therefore, it is of interest to investigate their complexes with a common acid and to compare their structural and electronic properties. Further insight into the comparison is obtained via examination of a broader series of SO_3 adducts, with focus on both ground-state physical properties *and* computationally derived binding energies. The results form a consistent picture in which the properties of these donor−acceptor systems can be readily discussed in terms of popular ideas of acidity and basicity.

* To whom correspondence should be addressed.

10.1021/jp010460u CCC: $20.00
Published on Web 05/11/2001

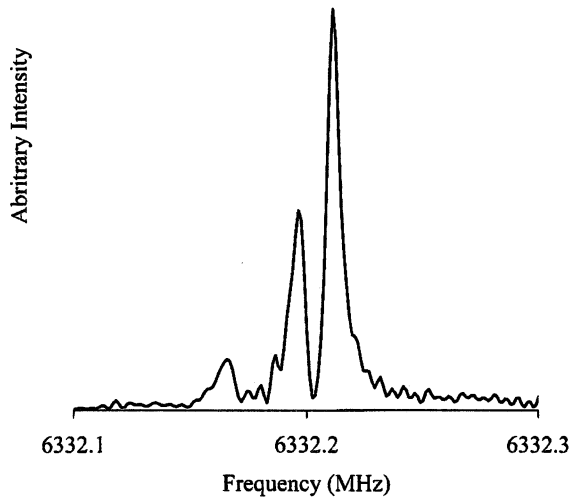

Figure 1. The three $\Delta F = 1$ components of the $4_{04} \leftarrow 3_{03}$ transition of meta-^{13}C substituted $C_5H_5N-{}^{32}SO_3$ observed in natural abundance. This spectrum represents 260 s of data collection time.

Experimental Section

Spectra were recorded using a Balle–Flygare type pulsed-nozzle Fourier transform microwave spectrometer[16] the details of which have been given previously.[17] Briefly, this system consists of two circular aluminum mirrors (84 cm radius of curvature) creating a Fabry–Perot cavity contained in a vacuum chamber evacuated by a 20″ diffusion pump. Adducts are created in situ by allowing the two species of interest to react in a supersonic expansion, which is aligned perpendicular to the axis of the cavity. Excitation is produced with a pulse of microwave radiation of about 2 μs in duration and, after a short time delay, the emission signal is heterodyne detected and Fourier transformed. The range of the instrument is 3 to 18 GHz and transition frequencies are measured with a typical accuracy of about 3 kHz.

For this experiment, a pulsed expansion-injection nozzle was used to generate the pyridine-SO_3 complex in situ. Pyridine was introduced by passing argon with a pressure of approximately 0.13 atm over a liquid sample and through a small stainless steel needle with an inner diameter of 0.012″. The needle was positioned to direct the pyridine into the early stages of a pulsed expansion of SO_3 in argon, which was prepared by passing argon at a pressure of approximately 2.2 atm over a solid sample of polymerized SO_3 held at 0° C. The ^{34}S, ^{15}N, and all ^{13}C species were observed in natural abundance, whereas an isotopically enriched sample was used to observe the perdeuterated isotopomer. A sample spectrum for the meta-^{13}C substituted derivative observed in natural abundance is shown in Figure 1, illustrating the good signal-to-noise ratios obtained even for rare isotopic forms.

Results

A-type rotational transitions were observed for $C_5H_5{}^{14}N-{}^{32}SO_3$, $C_5H_5{}^{14}N-{}^{34}SO_3$, $C_5H_5{}^{15}N-{}^{32}SO_3$, $C_5H_5{}^{14}N-{}^{32}SO_3$ with single ^{13}C substitution in the ortho, meta, and para positions, and $C_5D_5{}^{14}N-{}^{32}SO_3$. When present, ^{14}N hyperfine structure was observed and analyzed, except in the case of $C_5D_5{}^{14}N-{}^{32}SO_3$, where the presence of six quadrupolar nuclei severely complicates the spectrum. As a result, for this species, only the strongest component is reported as an approximate linecenter. Interestingly, however, in the $5_{05} \leftarrow 4_{04}$ transition the deuterium hyperfine structure is collapsed and the observed transitions can be fit to a hyperfine splitting pattern of a ^{14}N nucleus only, with a quadrupole coupling constant similar to that observed in the parent species. Because line intensities were significantly weaker for the less abundant isotopomers, observations were limited to a smaller number of transitions than for the parent species. Measured transitions for all isotopic species with resolved hyperfine structure are provided as Supporting Information. The observed frequencies were fit first to give the hyperfine free linecenters and quadrupole coupling constants, which are listed in Tables 1 and 2, respectively. Table 1 also

TABLE 1: Hyperfine-Free Linecenters for Observed Transitions of Pyridine-SO_3

	frequency (MHz)[a]	residual (MHz)[b]
	$C_5H_5{}^{14}N-{}^{32}SO_3$	
$1_{01}-2_{02}$	3205.378	0.002
$1_{10}-2_{11}$	3316.233	0.003
$1_{11}-2_{12}$	3098.067	0.002
$2_{02}-3_{03}$	4803.641	0.003
$2_{11}-3_{12}$	4973.229	0.001
$2_{12}-3_{13}$	4646.000	0.000
$2_{21}-3_{22}$	4810.724	0.003
$2_{20}-3_{21}$	4817.806	0.001
$3_{03}-4_{04}$	6396.608	0.002
$3_{12}-4_{13}$	6628.856	−0.006
$3_{13}-4_{14}$	6192.636	−0.005
$4_{04}-5_{05}$	7982.575	0.000
	$C_5H_5{}^{14}N-{}^{34}SO_3$	
$2_{02}-3_{03}$	4767.696	0.004
$2_{11}-3_{12}$	4934.663	0.004
$2_{12}-3_{13}$	4612.310	0.002
$3_{03}-4_{04}$	6348.932	−0.001
$3_{12}-4_{13}$	6577.498	−0.004
$3_{13}-4_{14}$	6147.777	−0.003
	o-$^{13}C\ C_4H_5{}^{14}N-{}^{32}SO_3$	
$2_{02}-3_{03}$	4791.213	0.005
$2_{11}-3_{12}$	4962.765	0.003
$2_{12}-3_{13}$	4632.087	0.003
$3_{03}-4_{04}$	6379.704	−0.001
$3_{12}-4_{13}$	6614.817	−0.004
$3_{13}-4_{14}$	6174.004	−0.003
	m-$^{13}C\ C_4H_5{}^{14}N-{}^{32}SO_3$	
$2_{02}-3_{03}$	4755.395	0.003
$2_{11}-3_{12}$	4924.435	0.004
$2_{12}-3_{13}$	4598.426	0.003
$3_{03}-4_{04}$	6332.198	0.000
$3_{12}-4_{13}$	6563.774	−0.004
$3_{13}-4_{14}$	6129.184	−0.002
	p-$^{13}C\ C_4H_5{}^{14}N-{}^{32}SO_3$	
$2_{02}-3_{03}$	4731.806	0.005
$2_{11}-3_{12}$	4896.160	−0.001
$2_{12}-3_{13}$	4578.665	0.003
$3_{03}-4_{04}$	6301.325	−0.002
$3_{12}-4_{13}$	6526.236	0.000
$3_{13}-4_{14}$	6102.978	−0.002
	$C_5H_5{}^{15}N-{}^{32}SO_3$	
$3_{03}-4_{04}$	6395.863	0.003
$3_{12}-4_{13}$	6628.045	−0.001
$3_{13}-4_{14}$	6191.947	−0.001
$4_{04}-5_{05}$	7981.649	−0.001
	$C_5D_5{}^{14}N-{}^{32}SO_3$	
$2_{02}-3_{03}$	4501.421	0.006
$2_{12}-3_{13}$	4336.280	0.011
$2_{11}-3_{12}$	4683.062	0.012
$3_{03}-4_{04}$	5990.537	0.005
$3_{13}-4_{14}$	5778.902	−0.012
$3_{12}-4_{13}$	6241.125	−0.013
$4_{04}-5_{05}$	7470.070	−0.002

[a] Estimated uncertainty is ±3 kHz, which was the typical standard error in the fits of the hyperfine structure used to obtain linecenters. [b] Residuals are from least-squares fits of the hyperfine-free linecenters to eq 1.

TABLE 2: Rotational and Quadrupole Coupling Constants for $C_5H_5N-SO_3$[a]

	$C_5H_5{}^{14}N-{}^{32}SO_3$	$C_5H_5{}^{14}N-{}^{34}SO_3$	$C_5H_5{}^{15}N-{}^{32}SO_3$	p-$^{13}CC_4H_5{}^{14}N-{}^{32}SO_3$
A'_z	5838.4(3)	5839.3(8)	5838.4(11)	5840.1(12)
B_y	856.3280(3)	849.4876(3)	856.2181(10)	842.6612(5)
C_z	747.2458(3)	742.0313(3)	747.1666(10)	736.8227(5)
eQq_{aa}	−1.5252(30)	−1.5218(60)		−1.539(44)
$[eQq_{bb} - eQq_{aa}]$	−0.1565(70)	−0.152(13)		−0.14(17)

	o-$^{13}CC_4H_5{}^{14}N-{}^{32}SO_3$	m-$^{13}CC_4H_5{}^{14}N-{}^{32}SO_3$	$C_5D_5{}^{14}N-{}^{32}SO_3$
A'_z*	5745.2(11)	5744.1(12)	4850.5(56)[b]
B_y*	854.8786(5)	848.0954(5)	809.6669(80)[b]
C_z	744.6464(5)	739.4198(5)	694.0625(80)
eQq_{aa}	−1.533(41)	−1.537(44)	
$[eQq_{bb} - eQq_{cc}]$	−0.12(13)	−0.10(17)	

[a] All values in MHz. Uncertainties are one standard error in the least-squares fits. [b] $A'_z{}^* = A_z'$ and $B^* = B_y$ for the perdeutero derivative.

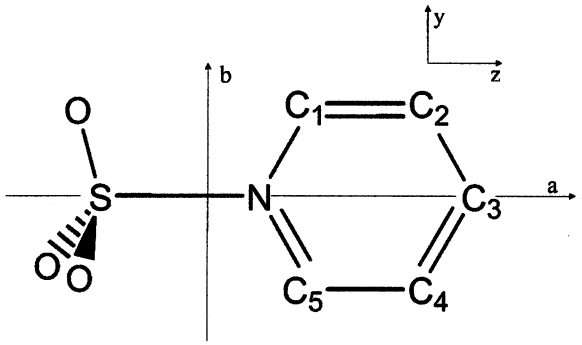

Figure 2. Atom labeling and definition of axes in py-SO_3.

includes data for the $C_5H_5{}^{15}N-{}^{32}SO_3$ and $C_5D_5{}^{14}N-{}^{32}SO_3$ species, for which preliminary fits of hyperfine structure were not performed. Only states corresponding to the ground internal rotor state of the SO_3 unit were observed, presumably due to effective cooling of the pyridine and SO_3 in the jet.

Linecenters followed the characteristic pattern for a rigid asymmetric rotor and were readily fit to the simplified Hamiltonian of eq 1, giving the effective rotational constants $A'_z{}^*$, $B_y{}^*$, and C_x[18,19] (see Figure 2 for axis labeling)

$$H = A'_z{}^* P_z^2 + B_y{}^* P_y^2 + C_x P_x^2 \quad (1)$$

Equation 1 is expected to apply for the ground internal rotor state ($m = 0$ of the SO_3 unit) in the absence of a significant barrier term. As a result of the internal rotation, however, the effective rotational constants $A'_z{}^*$ and $B_y{}^*$ differ from $h/8\pi^2 I_{aa}$ and $h/8\pi^2 I_{bb}$, respectively. Using the notation similar to Kreiner,[19] the prime indicates that the A rotational constant is perturbed by the internal rotation in all isotopic species and the asterisks indicate that both A and B will be further perturbed by off-axis isotopic substitution. For the parent isotopomer and those with on-axis or symmetrical substitution, only the A rotational constant is affected by internal rotation. In this case

$$A'_z{}^* = A'_z = (h/8\pi^2)/(I_z - I_\alpha) = (h/8\pi^2)/I_z \quad (2a)$$

and

$$B_y{}^* = B_y \quad (2b)$$

where $I_z = (h/8\pi^2)/A_z$ is the moment of inertia of the rigid complex about z, and I_α is the moment of inertia of the SO_3 unit about its symmetry axis at its distorted configuration in the complex.

For isotopic derivatives with off-axis substitution an additional correction is needed because the axis of internal rotation does not coincide with the a-axis of the complex. For these species

$$A'_z{}^* \cong A'_z [1 - \epsilon^2 I_\alpha / I_z] \quad (3a)$$

and

$$B_y{}^* \cong B_y [1 + \epsilon^2 I_\alpha / I_y] \quad (3b)$$

where ϵ is the angle (in radians) between the internal rotation axis and the principle inertial axis z. In both cases of off-axis substitution for this complex, ϵ is very small (0.16° and 0.40°), and the correction does not change the rotational constants within the precision that they are determined.

The effective rotational constants for the isotopic species studied are listed in Table 2. Residuals for the fitted linecenters are seen to be less than 6 kHz for the parent and all singly substituted derivatives and 13 kHz for the perdeuterated species. Several attempts were made to include centrifugal distortion terms but the resulting constants were only marginally determined statistically, and the improvement in the residuals of the fit was only slight. In light of these results and because the residuals in Table 1 are on the order of the estimated uncertainties for the linecenters, further attempts to fit the centrifugal distortion were not pursued. Because the complex has only a-type spectra, values of A are not well determined and consequently, their standard errors are several orders of magnitude higher than those for either B or C.

Computational Methods and Results

Ab initio geometry optimizations and energy calculations were performed for py-SO_3 and, for the purposes of comparison, for $(CH_3)_3N-SO_3$, H_3N-SO_3, CH_3CN-SO_3, HCCCN−SO_3, and HCN−SO_3 as well. Calculations for all species were done at both the MP2/aug-cc-pVDZ and the MP2/aug-cc-pVTZ levels using Molpro 2000.1.[20] Comparison of results obtained from both basis sets showed that geometries and energies for all complexes studied are reasonably converged, and values obtained from the MP2/aug-cc-pVTZ calculations are presented in Table 3. Binding energies were calculated as the difference between the optimized dimer energy and the sum of the optimized monomer energies, viz., $D_e = E(B-SO_3)_{opt} - [E(SO_3)_{opt} + E(B)_{opt}]$ (where B = $(CH_3)_3N$, py, NH_3, CH_3CN, HCCCN, or HCN). Zero point energies were not calculated, as the computed well depths provide a logical basis for comparison across the series. The equilibrium bond distances are also listed in Table 3 and are seen to fall in most cases to within 0.04 Å of the vibrationally averaged values determined experimentally. The N−S distances calculated for py-SO_3 and NH_3-SO_3 are somewhat farther from the experimental values (0.05 and 0.06

TABLE 3: Binding Energies and Bond Lengths for Complexes of SO_3[a]

	D_e (kcal/mol)	ΔD_e(cpc) (kcal/mol)	D_e(cpc) (kcal/mol)	ΔD_e(dist) (kcal/mol)	R(NS) [Å] theoretical	R(NS) [Å] experimental
$(CH_3)_3N-SO_3$	40.04	3.77	36.27	−11.34	1.951	1.912[b]
$C_5H_5N-SO_3$	28.40	2.87	25.53	−9.18	1.969	1.915[c]
NH_3-SO_3	21.36	1.81	19.55	−6.22	2.017	1.957[d]
CH_3CN-SO_3	10.22	1.19	9.03	−0.77	2.444	2.466[e]
$HCCCN-SO_3$	8.51	1.11	7.40	−0.42	2.525	2.568[f]
$HCN-SO_3$	8.23	0.98	7.25	−0.37	2.547	2.577[e]

[a] Calculated results at the MP2/aug-cc-pVTZ level/basis set. [b] Reference 4. [c] This work. [d] Reference 23. [e] Reference 24. [f] Reference 25.

Å, respectively), but the trend among the series of complexes is retained nonetheless.

To estimate the degree of basis set superposition error, further energy calculations were performed with the monomers held fixed at their geometries in the optimized complex, using first only the basis functions of the monomer (mb) and then the full basis of the dimer (db). The counterpoise correction[21] is the difference in the energy of the monomers calculated with the monomer and the full dimer basis, $\Delta D_e(\text{cpc}) = [E(SO_3)_{mb} + E(B)_{mb}] - [E(SO_3)_{db} + E(B)_{db}]$. The counterpoise correction decreases as the basis set increases, from 2.2 kcal/mol for cc-pVDZ to 2.1 kcal/mol for aug-cc-pVDZ to 1.0 kcal/mol for aug-cc-pVTZ for $HCN-SO_3$. However, it is nearly 4 kcal/mol with the aug-cc-pVTZ basis set for $(CH_3)_3N-SO_3$ which has nearly twice as many basis functions as $HCN-SO_3$. Although the counterpoise correction increases by nearly a factor of 4 across the series from $HCN-SO_3$ to $(CH_3)_3N-SO_3$, in all complexes it is roughly 10% of the binding energy. The calculated correction is subtracted from the initial binding energy, D_e, for each complex to give an improved estimate, D_e(cpc). Values of D_e(cpc) are also listed in Table 3. Because the counterpoise correction generally represents a maximum correction to the basis set superposition error, the true binding energies likely lie in the range between the counterpoise corrected and uncorrected values. The 19.6 kcal/mol binding energy obtained for the H_3N-SO_3 with the counterpoise correction is similar to the 19.1 kcal/mol value obtained by Wong, Wiberg, and Frisch.[22]

From the above calculations, we can also determine the energy associated with the distortion of the monomers upon complexation as $\Delta D_e(\text{dist}) = [E(SO_3)_{opt} + E(B)_{opt}] - [E(SO_3)_{mb} + E(B)_{mb}]$. As noted above, $E(X)_{opt}$ refers to the calculated energy of free X at its optimized geometry, and $E(X)_{mb}$ refers to the calculated energy of X in its distorted geometry in the complex, both obtained with the monomer basis set. This distortion energy is only a few tenths of a kcal/mol for $HCN-SO_3$, but several kcal/mol for py-SO_3 and $(CH_3)_3N-SO_3$, which are more tightly bound and undergo greater geometrical changes of the SO_3 unit upon complexation. Values of ΔD_e(dist) are also included in Table 3.

Structure Analysis

The observed asymmetric top spectrum and the isotope shifts confirm the expected geometry in which the pyridine ring is planar with its C_2 axis along the C_3 axis (the axis of internal rotation) of the SO_3 unit. As is evident in Figure 2, this symmetry axis is identically the a-axis of the complex for symmetrically substituted forms and very nearly the a-axis for the asymmetrically substituted derivatives. Preliminary analysis indicated the nitrogen−sulfur bond length to be about 1.9 Å, which is slightly longer than the sum of covalent radii for nitrogen and sulfur (1.74 Å). Although three isotopically substituted species certainly do not provide enough data to fit all parameters, initial attempts were made to determine the structure prior to the observation of the ^{13}C species. Past work on similar adducts has indicated that it is frequently sufficient to determine only the N−S distance, R(NS), and the NSO angle, α(NSO), while leaving the remaining internal structural parameters of the monomers fixed at their free-molecule values.[4,23,24] Because there are slight differences in the pyridine ring structure in the gas phase[26] and in the X-ray structure of the complex,[27] data were fit with the pyridine ring fixed at both its gas-phase structure and its structure in solid py-SO_3.[28] With either set of pyridine ring parameters, however, the fits were very poor, with residuals of several MHz in all of the B and C rotational constants included. The A rotational constants were not included, as they are strongly perturbed by rotation of the SO_3 unit. Indeed, we note that the values of A obtained for the complex were very nearly equal to those of free pyridine (rather than rigid py-SO_3), indicating the that internal rotation of the SO_3 moiety is either free or only slightly hindered.[29]

TABLE 4: Structural Parameters of $C_5H_5N-SO_3$

	fit I[a]	fit II	preferred structure[d]	Kraitchman
R(NS) [Å]	1.871879(32)	1.944786(32)	1.915 (1)	1.826
α(NSO) [deg]	98.3042(22)	99.6174(23)	98.91(2)	*e*
$R(N-C_1)$ [Å]	1.338[b]	1.332[c]	1.3409 (6)	1.379
$R(C_1-C_2)$ [Å]	1.394[b]	1.368[c]	1.3863 (3)	1.405
$R(C_2-C_3)$ [Å]	1.392[b]	1.370[c]	1.402 (6)	1.395
$<(C_1NC_5)$ [deg]	116.9[b]	121.9[c]	122.0(1)	117.4
$<(NC_1C_2)$ [deg]	123.8[b]	120.1[c]	120.55 (6)	122.3
$<(C_1C_2C_3)$ [deg]	118.5[b]	118.75[c]	118.6(1)	119.3
$R(N-C_3)$ [Å]	2.805	2.695	2.740	2.825
$R(S-C_3)$ [Å]	4.677	4.640	4.656	4.651

[a] Because the pyridine ring has C_{2v} symmetry in the gas-phase complex, $R(C_1-C_2) = R(C_5-C_4)$, $<(NC_1C_2) = <(NC_5C_4)$, etc. [b] Values fixed at the microwave structure of free pyridine in reference [26b]. [c] Values fixed at averages from $C_5H_5N-SO_3$ crystal structure in ref 27. [d] See text for discussion. [e] Not determined, as there was no oxygen substitution.

Following the observation of the ^{13}C substituted forms of the complex, similar fits varying only R(NS) and α(NSO) were attempted. The structural parameters derived from these fits are given in Table 4, where Fit I utilizes the structure of free pyridine and Fit II utilizes the ring structure observed in solid py-SO_3. Still, however, the resulting residuals were poor, with errors of approximately +1.5 MHz in all the B rotational constants and −2 MHz in all of the C rotational constants. Thus, it became apparent that additional parameters needed to be freed in the analysis.

The observations of the ^{15}N and ^{13}C isotopomers comprise a series of species in which all heavy atoms in the pyridine ring are substituted and from which, therefore, the heavy atom ring structure can be determined. Thus, another series of fits was done including as adjustable parameters all of the structural parameters in the pyridine ring with the exception of those pertaining to the positions of the hydrogens. Observation of only one ^{13}C isotopomer for substitution at each position in the ring

TABLE 5: Physical Properties Pertinent to Donor−Acceptor Complexes of SO_3

	R(NS)(Å) [α_{NSO}(deg)]	electron transfer	IE(eV)[a]	EA(eV)[a,b]	ΔE(eV)[c]	χ(eV)[b]	η(eV)[b]	$\Delta E_{\chi\eta}$(eV)[d]
SO_3			12.80[e]	1.70[f]		7.2	5.5	
$(CH_3)_3N-SO_3$	1.912(20)[g] [100.1(2)]	0.58[g]	8.54[h]	−4.8	6.8	1.5	6.3	6.1
$C_5H_5N-SO_3$	1.915(1)[i] [98.91(2)]	0.54[i]	9.66[j,k]	−0.59[l]	8.0	4.4[m]	5.0[m]	7.7
H_3N-SO_3	1.957(23)[n] [97.6(4)]	0.36[n]	10.85[o]	−5.6	9.2	2.6	8.2	9.1
CH_3CN-SO_3	2.466(16)[p] [92.0(7)]	0.16[p]	13.17[j,q]	−2.8	11.5	4.7	7.5	10.5
$HCCCN-SO_3$	2.568(8)[r] [91.9(3)]		13.54[j,q]	2.56[s]	11.8	7.2[t]	4.6[t]	10.1
$HCN-SO_3$	2.577(6)[p] [91.8(4)]	0.13[p]	14.01[j,u]	−2.3	12.3	5.7	8.0	12.0

[a] Values listed for complexes refer to the basic moiety. Ionization energies are vertical values. [b] Reference 7a, unless otherwise noted. [c] Energy difference between donor and acceptor orbitals, calculated from IE and EA values. [d] Energy difference between donor and acceptor orbitals calculated from χ and η. [e] Reference 37. [f] Reference 38. [g] Reference 4. [h] Reference 39. [i] This work. [j] Ionization from the nitrogen lone pair. [k] Reference 40. [l] Reference 41. [m] Reference 7d. [n] Reference 23. [o] Reference 42. [p] Reference 24. [q] Reference 43. [r] Reference 25. [s] Reference 44. [t] Calculated using $\chi = {}^1/_2$(IE + EA) and $\eta = {}^1/_2$(IE − EA). Following the convention of Reference 7a, the first ionization energy is used (11.75 eV from Reference 43). [u] Reference 45.

indicates that pyridine retains its C_{2v} symmetry in the complex and is not perturbed in the gas phase, as it is in the solid. It seems likely, therefore, that the slight asymmetry in the solid phase of the complex is due to crystal effects. Hydrogen distances and angles were kept fixed using parameters from the gas phase structure of free pyridine, as these values are consistent with the symmetry of the ring structure and are better determined than those in the solid. With the fits performed in this way, residuals of the fitted rotational constants were on the order of only tens of kilohertz, which represents a significant improvement over the earlier analysis. $R(C_2-C_3)$ and $\angle(C_1C_2C_3)$ were found to be highly correlated, however, and thus, the final analysis was done with $\angle(C_1C_2C_3)$ held fixed in separate fits at 118.5° (its value in free pyridine in the gas phase[26b]) and 118.75° (the average value in the X-ray crystal structure of the complex[27]). Similarly, fits were done with the S−O bond distance constrained to the gas-phase value of 1.4198 Å in free SO_3[30] and the average of the three distances observed in solid py-SO_3 (1.422 Å). The differences between the fits applying any of the above constraints were small, and the values reported under "Preferred Structure" of Table 4 are the corresponding averages, with error bars combined to reflect the full range of values obtained. The values of R(NS) and α(NSO) are seen to fall between those obtained from either of fits I or II.

Because of the ease of obtaining C_5D_5N, the fully deuterated species of the complex was observed to provide an additional confirmation of the structure. Including the rotational constants of this isotopomer in the structure fit results in a 0.006 Å longer NS distance with residuals for the deuterated species a factor of 3 larger than those of the parent and singly substituted species. These errors are small and may be due, at least in part, to uncertainty in the zero-point reduction of the C−H bonds upon deuteration (which would be compensated by a longer N−S distance in the fit) and perhaps to the somewhat larger uncertainties in the pyridine rotational constants themselves. Because determination of the true CH/D distance would require single-deuterium substitutions, the data from the fully deuterated species is not included in the final structure fit. It is worth noting, however, that the observed values of B and C for the perdeutero derivative differ from those calculated using the "Preferred Structure" by only 0.43 and 0.45 MHz respectively.[31]

As a further independent check of the structure, a Kraitchman analysis[18,32] was performed following the method of Kreiner,[19] which includes several corrections to account for the effects of internal rotation. Although the S−C_3 distance was found to be in agreement with the results of the least-squares fit, the individual distances R(NS) and R(N−C_3) differed by +0.09 Å and −0.09 Å, from those reported for the "Preferred Structure" of Table 4. This indicates that the primary difference between the two structures is in the location of the nitrogen atom. Upon closer examination, we observed that the nitrogen lies within approximately 0.3 Å of the center of mass of the complex, a situation notorious for producing inaccurate coordinates in the Kraitchman method.[18a] Moreover, a survey of the literature[33−36] revealed that the CNC angle in pyridinium complexes is typically in the 121° −128° range, comparable to that observed in solid py-SO_3 and that obtained for the preferred structure. Indeed, it has been noted previously[33] that an increase in the CNC angle of free pyridine is characteristic upon protonation, and the 117° value obtained from the Kraitchman analysis therefore would appear surprisingly low. Although comparisons with pyridinium complexes certainly do not provide a definitive basis for rejecting the Kraitchman structure of py-SO_3, they support the suspicion that the nitrogen coordinates are in error. Thus, the results of the least-squares fits are probably more reliable.

Discussion

Molecular Structure and Electronic Structure. Structural parameters for py-SO_3 are listed in Table 5 together with those of a number of related complexes. The nitrogen−sulfur bond length of 1.915(1) Å observed in gas-phase py-SO_3 is much shorter than the estimated van der Waals separation (2.9 Å) but is still slightly longer than the sum of the covalent radii (1.74 Å). Thus, the formation of the dative bond in py-SO_3 appears to be nearly, but not entirely, complete. The NSO bond angle of 99° corresponds to a significant out-of-plane distortion of the SO_3 unit and thus further indicates a substantial chemical interaction in the complex. The nitrogen−sulfur distance in the preferred structure is about 0.09 Å longer than the 1.829(5) Å value reported in the solid,[27] indicating that upon crystallization, the N−S bond undergoes a small but significant contraction. Although an effect of this size would be unusual for most covalent bonds, it is reasonable for a dative bond whose formation is incomplete. Indeed, bond length changes much greater than 0.09 Å have been reported for numerous partially bonded Lewis acid−base type complexes.[2] Nevertheless, we

note that a structure based on the (less favored) Kraitchman coordinates would indicate the nitrogen–sulfur distance is essentially the same in the gas and the solid phase.

The ^{14}N quadrupole coupling constant of the complex contains, at least in principle, information about the degree of electron transfer upon complexation. For free pyridine, analysis according to the method of Townes and Dailey,[18,46] gives

$$eQq_{aa} = [4a_s^2 - a/2 + (^1/_2 - 2a_s^2)b](eQq_{210}) \quad (5a)$$

and

$$[eQq_{bb} - eQq_{cc}] = (^3/_2)(b - a)(eQq_{210}) \quad (5b)$$

where a and b are the populations of the π and σ orbitals in the nitrogen–carbon bonds, respectively, and a_s^2 is the amount of s-character in each of the $\sim sp^2$ hybrid orbitals of nitrogen used to form the N–C σ bonds. eQq_{210} is the quadrupole coupling constant for a single $2p_z$ electron in atomic nitrogen, estimated to be −9.0 MHz.[47] Equations 5 are equivalent to those given by Lucken,[47] but differ slightly in notation. The value of a_s^2 can be obtained, as usual, from the C_1NC_5 bond angle, θ, using the relation

$$a_s^2 = \cos\theta/(\cos\theta - 1) \quad (6)$$

For py-SO_3, the wave function for the dative bond, ψ_D, may be approximated as a normalized linear combination of the donor and acceptor orbitals, $\phi(N)$ and $\phi(SO_3)$, respectively, viz

$$\psi_D = \alpha\phi(N) + \beta\phi(SO_3) \quad (7)$$

With this form, it is straightforward to show that the differences in quadrupole coupling constants between free pyridine[26c] and those of the complex are given by

$$\Delta(eQq_{aa}) \equiv [eQq_{aa}(\text{complex}) - eQq_{aa}(\text{pyridine})] = 4a_s^2(\alpha^2 - 1)(eQq_{210}) + (^1/_2)(a - a')(eQq_{210}) - (^1/_2)(b - b')(1-4a_s^2)(eQq_{210}) \quad (8a)$$

and

$$\Delta(eQq_{bb} - eQq_{cc}) \equiv \{[eQq_{bb} - eQq_{cc}](\text{complex}) - [eQq_{bb} - eQq_{cc}](\text{pyridine})\} = (^3/_2)(eQq_{210})[(a - a') - (b - b')] \quad (8b)$$

Here, the unprimed and primed values of a and b refer to the π and σ populations before and after complexation, respectively. Because $a \cong a'$ and $b \cong b'$, the change in eQq_{aa} upon complexation depends primarily on α and is relatively stable with respect to small changes in electron populations in the carbon–nitrogen bonds. On the other hand, note that the change in $[eQq_{bb} - eQq_{cc}]$ depends strongly and exclusively on the small differences $(a - a')$ and $(b - b')$. This dependence is apparent from the data presented above, for if $a = a'$ and $b = b'$, the value of $[eQq_{bb} - eQq_{cc}]$ of the complex equals that of free pyridine. Yet, using the value of $[eQq_{bb} - eQq_{cc}] = -2.014(5)$ MHz for free pyridine,[26c] the experimental ratio of $[eQq_{bb} - eQq_{cc}]$(pyridine)/$[eQq_{bb} - eQq_{cc}]$(complex) is approximately 13. With the value of $\theta = 122.0°$ given in Table 4, we obtain $a_s^2 = 0.3464$ for py-SO_3, and, using the observed value of $eQq_{aa}(^{14}N)$ for the parent isotopic form in eq 8a, $\alpha^2 = 0.73$. Invoking the usual neglect of overlap (i.e., assuming $\alpha^2 + \beta^2 \cong 1$) gives $n = 2\beta^2 \cong 2(1-\alpha^2) = 0.54\ e$, which is interpreted as the number of electrons transferred upon complexation.[48]

Values of n for complexes of SO_3 are also given in Table 5, where it is satisfying to observe that a decrease in N–S bond length is accompanied by a monotonic increase in electron transfer. However, although this trend is both clear and chemically sensible, the absolute numbers should not be regarded as quantitative for several reasons. The Townes and Dailey analysis, for example, contains many approximations,[18,46,47] and the form of the dative bond wave function expressed in eq 7 is extremely crude. In addition, the definition of electron transfer is by no means unique.[49] Interestingly, previous examination of both Mulliken and NPA population analyses of these systems also indicated an increasing degree of electron transfer as the N–S bond length shortens.[5] The absolute values, however, were found to be significantly smaller than those derived from hyperfine structure. As is usually the case in the interpretation of electron populations, it is the relative, rather than the absolute, values which are most significant.

A critical approximation inherent in the above determination of n is the neglect of overlap between $\phi(N)$ and $\phi(SO_3)$. Within the usual approximations of the Townes and Dailey analysis, it is α^2 that is determined directly from the quadrupole coupling constants, whereas subsequent calculation of $2\beta^2$ requires either knowledge or neglect of the overlap integral, $S \equiv \int\phi(N)\phi(SO_3)d\tau$. In this regard, it is interesting to note that the inclusion of an overlap integral as small as 0.1 into the normalization condition for Ψ_D reduces the 0.54 e value of n quoted above for py-SO_3 to only 0.39 e. Further increases in S result in a continued drop in n. Thus, although often ignored, the overlap integral has a significant effect on the estimation of charge transfer from hyperfine structure. Indeed, it is tempting to speculate that its effect may account, at least in part, for the apparent overestimation relative to population analyses.

Although the value of the overlap integral will not, in general, be simple to obtain, a slight clarification in interpretation of the electron transfer values readily circumvents the problem. In particular, we note that with the inclusion of S, the tabulated values of $n = 2(1 - \alpha^2)$ are equal to $2\beta^2 + 4\alpha\beta S$, which represents the population on the acid plus that in the shared bonding region. Thus, the "electron transfer" values listed in Table 5 are not the amount of charge transferred to the acid per se, but are better interpreted as the charge transferred *away* from the base. Such an interpretation does not specify how the transferred electrons are partitioned between the acid and bonding region, but nevertheless conveys a sense for the degree to which a Lewis acid–base reaction has occurred between the moieties.

Correlation of Physical Properties with Orbital Energy Gaps. The increase in charge transfer and the geometrical changes observed for the complexes in Table 5 suggest a progressive advancement of the dative bond between HCN–SO_3 and $(CH_3)_3N-SO_3$. The correlation between these properties, however, does not, in itself, illuminate the factors that determine the order of these compounds within the series. As noted in the Introduction, the intrinsic strength and compatibility of the acid and base would appear to be important in determining the degree of dative interaction. In this light, therefore, it is of interest to identify specific physical properties of the donor and acceptor which combine to produce the variations observed among their respective complexes.

In the language of the HSAB theory, electron transfer between the acid and base arises from the covalent ("soft–soft") portion

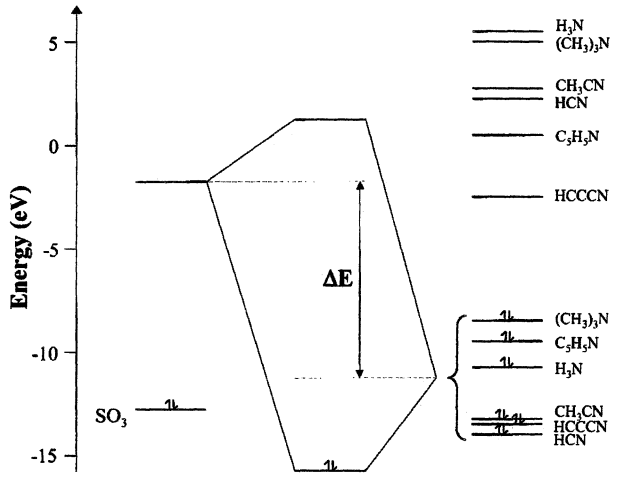

Figure 3. Orbital energy diagram for SO_3 and its basic binding partners, estimated from electron affinity and ionization energy data. Energies of the donor and acceptor orbitals are drawn to scale but the resulting orbitals of the complex are not.

of the donor–acceptor interaction. Thus, to the extent that bonding arises from mixing of the donor and acceptor orbitals, it is not unreasonable to expect that the degree of interaction across a series of related systems should correlate with the energy gap between those orbitals. While, strictly speaking, it is the bond *energy* that forms the basis for most measures of acid–base interaction strength, a smooth evolution of physical properties of the complexes between van der Waals and chemical interactions would not be unexpected. Moreover, insofar as electron transfer is concerned, the simple wave function written in eq 7 expresses the orbital mixing directly and, indeed, is identical in form to that used by Klopman in his treatment of donor–acceptor interactions.[12] Thus, the electron-transfer values derived from nuclear hyperfine structure provide, in a sense, a direct measure of the covalent portion of the interaction and may be expected to correlate with the energy difference between the donor and acceptor orbitals.

To test for such a correlation, orbital energies for the donor orbitals (the nitrogen lone pairs) and acceptor orbital (LUMO of SO_3) were estimated from experimental values of the ionization energies and electron affinities using Koopmans' theorem.[50] The resulting orbital energy gaps, ΔE, are given in Table 5, as are the ionization energies (IEs) and electron affinities (EAs) of the species of interest. An energy diagram is also presented in Figure 3. The ionization energies are, in some cases, the first ionization energy of the molecules. However, close examination reveals that the orbitals corresponding to the first IE are not always the same as those used in the donor–acceptor interaction. Specifically, in the case of the nitriles, it is the π orbital, not the lone pair, which corresponds to the first ionization energy. Thus, care has been taken in compiling Table 5 to use ionization energies pertinent to the orbitals involved in dative bond formation. Vertical values, which are appropriate for use with Koopmans' theorem, have been used for the ionization energies.

Figure 4 displays a plot of the number of electrons transferred (determined from nuclear hyperfine structure) against the energy gap between the donor and acceptor orbitals. The solid circles joined by a solid line utilize energy gaps determined by the method described above. The open circles joined by a dashed line are those derived from hardness and electronegativity parameters, as described below. Similar plots are presented in Figure 5, in which the nitrogen–sulfur bond length is displayed as a function of energy gap. Note that for both sets of data, the

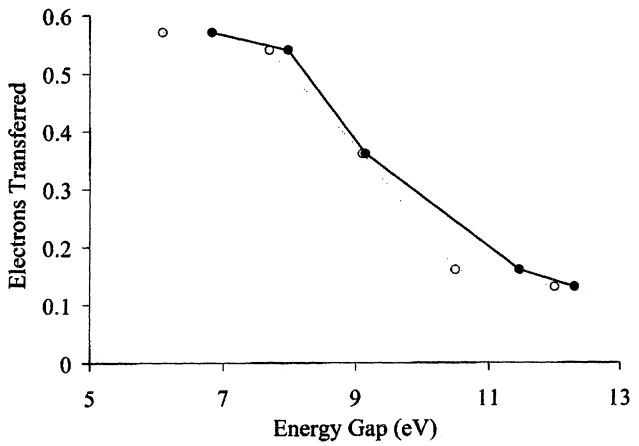

Figure 4. Electron-transfer values, calculated from the ^{14}N quadrupole coupling constants, vs the energy gap between the lone pair of the donor and the LUMO of the acceptor for complexes of SO_3 with several nitrogen-containing bases. Data for this plot are found in Table 5. Solid points represent energy differences calculated directly from IE and EA data (ΔE). Open points represent energy differences estimated from hardness and electronegativity values ($\Delta E_{\chi\eta}$). Lines are drawn for ease of visualization but have no fundamental significance.

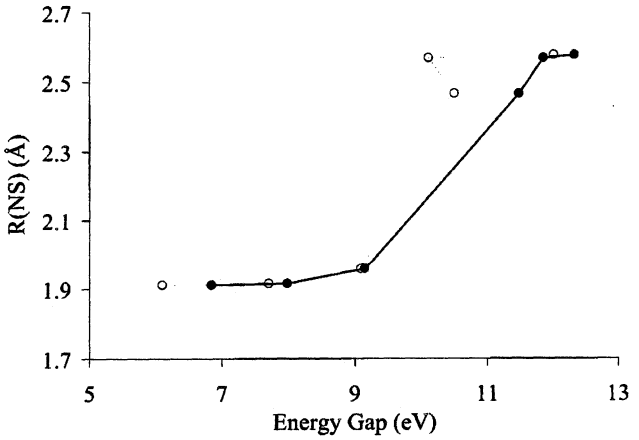

Figure 5. Gas-phase N–S bond distance vs the energy gap between the lone pair of the donor and the LUMO of the acceptor for complexes of SO_3 with several nitrogen-containing bases. Data for this plot is found in Table 5. Solid points represent energy differences calculated directly from IE and EA data (ΔE). Open points represent energy differences estimated from hardness and electronegativity values ($\Delta E_{\chi\eta}$). Lines drawn are for ease of visualization but have no fundamental significance.

lines are drawn for ease of visualization but have no fundamental significance.

The monotonic variation in electron transfer with donor–acceptor energy gap is apparent in Figure 4. For the bond lengths shown in Figure 5, a correlation is also suggested, though it is perhaps less clear, as the distances are more clustered at long and short values. Nevertheless, it appears that the orbital energy gap is indeed a useful, fundamental parameter with which simple physical properties of these complexes correlate. The calculated binding energies listed in Table 3 are also seen to increase from $HCN–SO_3$ to $(CH_3)_3N–SO_3$, consistent with a strengthening of the donor–acceptor bond as the orbital energy gap decreases.

It should be noted that orbital energies derived from ionization energies are generally more accurate than those obtained from electron affinities.[51,52] Thus, the energy values for the lone pair orbitals of the base are probably significantly better than that of the LUMO of SO_3. Nevertheless, the latter enters into the energy gaps for all members of the series as a constant offset and thus, any impropriety in the application of Koopmans'

theorem to EA values does not impact on the trend across the series. Indeed, a correlation with energy gap is equivalent in this context to a correlation with IE of the base. We prefer, however, to plot energy gap, as it is related in a more fundamental way to basic ideas of chemical bonding.

Correlations involving orbital energies are certainly not new. Indeed, the stabilization of "soft−soft" interactions in the HSAB theory arises from small energy gaps between the donor and acceptor orbitals.[7,12] The theory of weak charge transfer complexes, developed by Mulliken in 1952[14] also considers simple ideas of mixing between the donor and the acceptor orbitals and arrives at a correlation between donor ionization potential and the frequency of the donor-to-acceptor charge transfer band. The use of ionization energies to establish the correlation of Figures 4 and 5 is very similar in this regard. However, rather than interpreting the frequency of the charge transfer absorption, as in the Mulliken theory, the focus is on the physical properties of the ground electronic state. A similar result has recently been reported by Legon and co-workers[53] for complexes containing BrCl and ICl, in which charge transfer was correlated with the ionization potential of the basic binding partner. The results shown in Figure 4, however, cover a larger range, encompassing both relatively weak interactions (such as in $HCN-SO_3$) and more fully formed chemical bonds (such as in $(CH_3)_3N-SO_3$). This feature of the data set accounts for the somewhat different shapes of the resulting curves, which are sigmoidal in Figure 4 but exponential in the weak-bonding limit probed by Legon.

In light of the strong connections to the HSAB theory, we also considered the possibility that the hardness and electronegativity parameters tabulated by Pearson and Parr might be useful for generating the results shown in Figures 4 and 5. Values for the species of interest here are also given in Table 5. Pearson and Parr have argued[13] that the hardness, η, and the electronegativity, χ, are approximately given by $(\epsilon_{LUMO} - \epsilon_{HOMO})/2$ and $(\epsilon_{LUMO} + \epsilon_{HOMO})/2$, respectively, where ϵ_{LUMO} and ϵ_{HOMO} are the energies for the lowest unoccupied and highest occupied molecular orbitals, respectively. Thus, the energy gap between the donor and acceptor orbitals is simply $\Delta E_{\chi\eta} = [\eta(\text{acceptor}) + \eta(\text{donor})] - [\chi(\text{acceptor}) - \chi(\text{donor})]$. Energy gaps obtained in this way are also listed in Table 5 and the open circles in Figures 4 and 5 utilize these values. In the case of electron transfer, it is clear that the primary effect is a horizontal translation of the curve. For the bond length, however, the correlation is lost for the complexes of HCN and CH_3CN, for which the first ionization energy (used to derive the hardness and electronegativity parameters) is inappropriate, as described above. The overall horizontal translation of the curves arises because, although we have been careful to use only vertical IP's, the Pearson−Parr parameters do not distinguish between vertical and adiabatic values.

Summary

The complex formed from pyridine and SO_3 has been investigated in the gas phase. On the basis of structural evidence, the system is a Lewis acid−base type complex, in which the formation of the electron pair donor−acceptor bond is nearly, but not entirely, complete. The pyridine ring undergoes small but measurable changes in structure upon complexation, and the SO_3 subunit acts as a free or nearly free internal rotor within the adduct. Nuclear hyperfine structure indicates a transfer of about 0.54 electrons away from the pyridine moiety upon complexation.

These results, combined with similar data for the series of complexes, $B-SO_3$ (B = HCN, HCCCN, CH_3CN, H_3N, C_5H_5N, and $(CH_3)_3N$), offer a broader view of the formation of partial donor−acceptor bonds. In particular, physical properties such as N−S bond length and degree of electron transfer are shown to correlate with the energy difference between the nitrogen lone pair orbital and the LUMO of the SO_3. In the language of the theory of hard and soft acids and bases, these energy gaps are closely related to the soft−soft part of the interaction, which involves direct mixing of the donor and acceptor orbitals. Thus, the soft−soft interactions appear to dominate the variations in structure and bonding across the series. Hardness and electronegativity parameters (η and χ, respectively) are somewhat useful in predicting the position of a complex in the series but irregularities can arise, especially when the first ionization energy of the donor does not correspond to removal of an electron in the lone pair. Thus, orbital energy gaps estimated directly from ionization energy and electron affinity data for the relevant orbitals are more reliable.

Ab initio calculations of the binding energies for the above series of complexes vary from only 7.3 kcal/mol for $HCN-SO_3$ to 36.3 kcal/mol for $(CH_3)N-SO_3$ in the gas phase, and also increase as the donor and acceptor orbitals approach one another in energy. This observation is also in accord with a simple picture of soft−soft acid−base interactions.

Acknowledgment. This work was supported by the National Science Foundation; the donors of the Petroleum Research Fund, administered by the American Chemical Society; and the Minnesota Supercomputer Institute. We are especially grateful to Dr. Kelly Higgins for help in computing the binding energies.

Supporting Information Available: Tables of transition frequencies. This material is available free of charge via the Internet at http://pubs.acs.org.

References and Notes

(1) See, for example: (a) Hargittai, M.; Hargittai, I., *The Molecular Geometries of Coordination Compounds in the Vapour Phase*; Elsevier: Amsterdam, 1977. (b) *Spectroscopy and Structure of Molecular Complexes*, Yarwood, J., Ed., Plenum: London, 1973. (c) Mulliken, R. S.; Person, W. B., *Molecular Complexes. A Lecture and Reprint Volume*; Wiley: New York, 1969. (d) Satchell, D. P. N.; Satchell, R. S. *Q. Rev. Chem. Soc.* **1971**, *25*, 171. (e) Hargittai, M.; Hargittai, I. *Phys. Chem. Minerals* **1987**, 14, 413. (f) Pyykkö, P. *Chem. Rev.* **1997**, *97*, 597. (g) Haaland, A. *Angew Chem., Int Ed. Engl.* **1989**, *28*, 992. (h) Gal, J.-F.; Maria, P.-C. *Prog. Phys. Org. Chem.* **1990**, *17*, 159.

(2) (a) Leopold, K. R. In *Advances in Molecular Structure Research*; Hargittai, M., Hargittai, I., Eds.; JAI Press: Greenwich, CT, 1996; Vol. 2, p 103. (b) Leopold, K. R. Canagaratna, M.; Phillips, J. A. *Acc. Chem. Res.* **1997**, *30*, 57.

(3) Canagaratna, M.; Ott, M. E.; Leopold, K. R. *Chem. Phys. Lett.* **1997**, *281*, 63.

(4) Fiacco, D. L.; Toro, A.; Leopold, K. R. *Inorg. Chem.* **2000**, *39*, 37.

(5) Fiacco, D. L.; Mo, Y.; Hunt, S. W.; Ott, M. E.; Roberts, A.; Leopold, K. R. *J. Phys. Chem. A*, **2001**, *105*, 484.

(6) (a) Drago, R. S.; Wayland, B. B. *J. Am. Chem. Soc.* **1965**, *87*, 3571. (b) Drago, R. S. *Structure and Bonding* **1973**, *15*, 73.

(7) (a) Pearson, R. G. *Chemical Hardness*; Wiley-VCH: Weinheim, 1997. (b) Pearson, R. G. *J. Am. Chem. Soc.* **1963**, *85*, 3533. (c) Pearson, R. G. *Hard and Soft Acids and Bases*; Dowden, Hutchinson, & Ross: Stroudsburg, PA, 1973. (d) Pearson, R. G. *Inorg. Chem.* **1988**, *27*, 734.

(8) Schwarzenbach, G.; *Adv. Inorg. Che. Radiochem.* **1961**, *3*, 257.

(9) Ahrland, S.; Chatt, J.; Davies, N. R. *Quart. Rev. (London)* **1958**, *12*, 255.

(10) Edwards, J. O. *J. Am. Chem. Soc.* **1954**, *76*, 1540.

(11) See, for example (a) Jonas, V.; Frenking, G.; Reetz, M. T. *J. Am. Chem. Soc.* **1994**, *116*, 8741. (b) Brinck, T. *J. Phys. Chem.* **1997**, *101*, 3408. (c) Glendening, E. D.; Streitwieser, *J. Chem. Phys.* **1994**, *100*, 2900. (d) Branchadell, V.; Sbai, A.; Oliva, A. *J. Phys. Chem.* **1995**, *99*, 6472. (e) Skancke, A.; Skancke, P. N. *J. Phys. Chem.* **1996**, *100*, 15 079. (f) Fradera,

X.; Austen, M. A.; Bader, R. F. W. *J. Phys. Chem. A* **1999**, *103*, 304. (g) Rincón, L.; Almeida, R. *J. Phys. Chem. A* **1998**, *102*, 9244. (h) Umeyama, H.; Morokuma, K. *J. Am. Chem. Soc.* **1976**, *98*, 7208.

(12) Klopman, G. *J. Am. Chem. Soc.* **1968**, *90*, 223.

(13) Parr, R. G.; Pearson, R. G. *J. Am. Chem. Soc.* **1983**, *105*, 7512.

(14) Mulliken, R. S. *J. Am. Chem. Soc.* **1952**, *74*, 811.

(15) Lias, S. G.; Bartmess, J. E.; Liebman, J. F.; Holmes, J. L.; Levin, R. D.; Mallard, W. G. *J. Phys. Chem. Ref. Data* **1988**, 17. suppl. #1.

(16) Balle, T. J.; Flygare, W. H. *Rev. Sci. Instrum.* **1981**, *52*, 33.

(17) (a) Phillips, J. A.; Canagaratna, H.; Goodfriend, H.; Grushow, A.; Almlöf, J.; Leopold, K. R. *J. Am. Chem. Soc.* **1995**, *117*, 12549. (b) Phillips, J. A. Ph.D. Thesis, University of Minnesota 1996.

(18) (a) Gordy, W.; Cook, R. L. *Microwave Molecular Spectra*; Wiley: New York, 1984. (b) Townes, C. H.; Schawlow, A. L. *Microwave Spectroscopy*; Dover: New York, 1975.

(19) Kreiner, W. A.; Rudolph, H. D.; Tan, B. T. *J. Mol. Spectrosc.* **1973**, *48*, 86.

(20) (a) MOLPRO is a package of ab initio programs written by Werner, H.-J.; Knowles, P. J., with contributions from Amos, R. D.; Bernhardsson, A.; Berning, A.; Celani, P.; Cooper, D. L.; Deegan, M. J. O.; Dobbyn, A. J.; Eckert, F.; Hampel, C.; Hetzer, G.; Korona, T.; Lindh, R.; Lloyd, A. W.; McNicholas, S. J.; Manby, F. R.; Meyer, W.; Mura, M. E.; Nicklass, A.; Palmieri, P.; Pitzer, R.; Rauhut, G.; Schütz, M.; Stoll, H.; Stone, A. J.; Tarroni, R.; Thorsteinsson, T. (b) Hampel, C.; Peterson, K.; Werner, H.-J. *Chem. Phys. Lett.* **1992**, *190*, 1, and references therein.

(21) (a) Boys, S. F.; Bernardi, F. *Mol. Phys.* **1970**, *19*, 553. (a) van Lenthe, J. H.; van Duijneveldt-van de Rijdt, J. G. C. M.; van Duijneveldt, F. B. *Ab Initio Methods in Quantum Chemistry-II*, Lawley, K. P.; Ed.; Wiley: 1987; p 521, and references therein.

(22) Wong, M. W.; Wiberg, K. B.; Frisch, M. J. *J. Am. Chem. Soc.* **1992**, *114*, 523.

(23) Canagaratna, M.; Phillips, J. A.; Goodfriend, H.; Leopold, K. R. *J. Am. Chem. Soc.* **1996**, *118*, 5290.

(24) Burns, W. A.; Phillips, J. A.; Canagaratna, M.; Goodfriend, H.; Leopold, K. R. *J. Phys. Chem. A* **1999**, *103*, 7445.

(25) Hunt, S. W.; Fiacco, D. L.; Craddock, M.; Leopold, K. R., manuscript in preparation.

(26) (a) Bak, B.; Hansen-Nygaard, L.; Rastrup-Andersen, J. *J. Mol. Spectrosc.* **1958**, 2, 361. (b) Sørensen, G. O.; Mahler, L.; Rastrup-Andersen, N. *J. Mol. Struct.* **1974**, *20*, 119. (c) Heineking, N.; Dreizler, H.; Schwarz, R. Z. *Naturforsch. A* **1986**, *41*, 1210.

(27) Brownstein, S.; Gabe, E.; Lee, F.; Louie, B. *J. Org. Chem.* **1988**, *53*, 951.

(28) Because the pyridine ring in crystalline py-SO_3 is not of strictly C_{2v} symmetry, average values of the corresponding angles and distances were used for the fits employing solid-state values.

(29) Free rotation of the SO_3 unit along the a-axis of the complex should yield A'_z rotational constants equal to those of free pyridine. The fit values of A'_z differ by approximately 3.4% from the values for free pyridine. If the pyridine A rotational constant is recalculated using the structural parameters determined within the complex, this value is reduced by 2.6%. The differences may result from a small barrier to internal rotation and/or propagation of the errors in the fitted structural parameters through the calculation of A.

(30) Kaldor, A.; Maki, A. *J. Mol. Struct.* **1973**, *15*, 123.

(31) This may be compared with similar calculations for B and C of the parent derivative, which differ from the observed values by 0.13 and 0.09 MHz, respectively.

(32) Kraitchman, J. *Am. J. Phys.* **1953**, *21*, 17.

(33) Boenigk, D.; Mootz, D. *J. Am. Chem. Soc.* **1988**, *110*, 2135.

(34) Rérat, P. C. *Acta Crystallogr.* **1962**, *15*, 427.

(35) Rogers, R. D.; Bauer, C. B. *J. Chem. Crystallography* **1994**, *24*, 285.

(36) For details, see: Hunt, S. W.; Ph.D. Thesis, University of Minnesota, in preparation.

(37) Lias, S. G. "*Ionization Energy Evaluation*" in **NIST Chemistry WebBook, NIST Standard Reference Database Number 69**, Eds. Mallard, W. G.; Lindstrom, P. J.; November, **1998**, National Institute of Standards and Technology, Gaithersburg, MD, 20899 (*http://webbook.nist.gov*).

(38) Rothe, E. W.; Tang, S. Y.; Reck, G. P. *J. Chem. Phys.* **1975**, *62*, 3829.

(39) Elbel, S.; Dieck, H. T.; Demuth, R. *J. Fluorine Chem.* **1982**, *19*, 349.

(40) Utsunomiya, C.; Kobayashi, T.; Nagakura, S. *Bull. Chem. Soc. Jpn.* **1978**, *51*, 3482.

(41) Burrow, P. D.; Ashe, A. J.; III.; Bellville, D. J.; Jordan, K. D. *J. Am. Chem. Soc.* **1982**, *104*, 425.

(42) Kimura, K.; Katsumata, S.; Achiba, Y.; Yamazaki, T.; Iwata, S. *Handbook of He I Photoelectron Spectra of Fundamental Organic Molecules*; Halsted Press: New York, 1981.

(43) Åsbrink, L.; von Niessen, W.; Bieri, G. *J. Electron Spectrosc. Relat. Phenom.* **1980**, *21*, 93.

(44) Bartmess, J. E., "*Negative Ion Energetics Data*", in **NIST Chemistry WebBook, NIST Standard Reference Database Number 69**, Eds. Mallard, W. G.; Lindstrom, November **1998**, National Institute of Standards and Technology, Gaithersburg, MD 20899 (*http://webbook.nist.gov*).

(45) Kreile, J.; Schweig, A.; Thiel, W. *Chem. Phys. Lett.* **1982**, *87*, 473.

(46) Townes, C. H.; Dailey, B. P. *J. Chem. Phys.* **1949**, *17*, 782.

(47) Lucken, E. A. C. *Nuclear Quadrupole Coupling Constants*; Academic Press: New York, 1969.

(48) Because $\Delta(eQq_{bb} - eQq_{cc})$ depends only on $(\Delta a - \Delta b)$, Δa and Δb cannot be independently determined. Thus, it is not possible to use eq 8a to provide a value of α which is corrected for the effects of changing σ and π populations. We note, however, that if Δa were zero, the value of Δb necessary to account for the observed $\Delta(eQq_{bb} - eQq_{cc})$ (eq 8b) raises the calculated value of n from 0.54 e to 0.58 e. Similarly, if Δb were zero, the value of Δa needed to account for the observed $\Delta(eQq_{bb} - eQq_{cc})$ changes n to a value of 0.44 e.

(49) See, for example, Bachrach, S. M. In *Reviews in Computational Chemistry*; Lipkowitz, K. B., Boyd, D. B., Eds.;, VCH Publishers: New York, Vol. V, 1994; p 171.

(50) Koopmans, A. *Physica* **1933**, *1*, 104.

(51) Simons, J.; Jordan, K. D. *Chem. Rev.* **1987**, *87*, 535.

(52) Eland, J. H. D. *Photoelectron Spectroscopy*, 2nd ed.; Butterworth: London, 1984.

(53) Legon, A. C.; Thumwood, J. M. A.; Waclawik, E. R. *J. Chem. Phys.* **2000**, *113*, 5278.